Polymer Chemistry

Accepted Manuscript

This is an *Accepted Manuscript*, which has been through the Royal Society of Chemistry peer review process and has been accepted for publication.

Accepted Manuscripts are published online shortly after acceptance, before technical editing, formatting and proof reading. Using this free service, authors can make their results available to the community, in citable form, before we publish the edited article. We will replace this *Accepted Manuscript* with the edited and formatted *Advance Article* as soon as it is available.

You can find more information about *Accepted Manuscripts* in the Information for Authors.

Please note that technical editing may introduce minor changes to the text and/or graphics, which may alter content. The journal's standard Terms & Conditions and the Ethical guidelines still apply. In no event shall the Royal Society of Chemistry be held responsible for any errors or omissions in this *Accepted Manuscript* or any consequences arising from the use of any information it contains.

ROYAL SOCIETY OF CHEMISTRY

www.rsc.org/polymers

Journal Name

ARTICLE

Side-Chain Engineering Approach to Solvent-Resistant Semiconducting Polymer Thin Films

Received 00th January 20xx,
Accepted 00th January 20xx

DOI: 10.1039/x0xx00000x

www.rsc.org/

Zi-Hao Guo,[a] Na Ai,[c] Connor Ryan McBroom[a],Tianyu Yuan,[a,b]Yen-Hao Lin,[a]Michael Roders,[d]Congzhi Zhu,[a]Alexander Ayzner,[d]Jian Pei*[c] and Lei Fang*[a,b]

Side-chain manipulation of isoindigo-thiophene derived conjugated polymers was achieved by statistical copolymerization of two different isoindigo monomers decorated with *t*-Boc group and polyisobutylene chain, respectively. The long polyisobutylene side-chain ensured solution-processability of the polymers while the *t*-Boc group served as a cleavable H-bond inhibitor. By post-film-casting thermal treatment, the *t*-Boc group could be removed efficiently to generate a H-bond cross-linked polymer network, which demonstrated excellent solvent resistance. Organic field-effect transistor devices of these thin films demonstrated retained electronic properties after being immersed in organic solvents. By taking advantage of the post-annealing solvent resistant feature, multilayered films of the polymers could be fabricated using multiple "casting-annealing-casting-annealing" cycles.

Introduction

In the past two decades, the research of semiconducting organic polymer materials and their applications in optical/electronic devices, such as organic light-emitting diodes (OLED)[1–3], organic field-effect transistors (OFETs)[4–6], and organic photovoltaics (OPV)[7–9], have drawn tremendous efforts from multiple disciplines of science and engineering. So far, OFETs reached excellent performance comparable to amorphous silicon[4], while the power conversion efficiency (PCE) of OPV devices has surpassed 10%[9].Compared to the inorganic semiconducting materials, organic materials possess the advantages of low-cost fabrication, potentially flexible and stretchable mechanical properties, and light-weight construction.[10] One of the main advantages of semiconducting organic materials is the low-cost solution phase processability.[11] Flexible side-chains are often introduced to the usually rigid backbone of semiconducting organic polymers to afford well-solubilizing materials that can be easily processed from solution.[12] Although this strategy works well in proof-of-concept devices, its practical application is limited because the casted thin films of such materials cannot resist another step of solvent treatment. This problem imposes challenges in multi-layer solution process of functional device and in applications that require direct contact of the active layer with solvents/solutions (such as sensors).

In this context, it is necessary to develop materials that allow for solution processing but the corresponding films are solvent resistant. This goal can be achieved by introducing solubilizing groups that are cleavable through post-process treatment.[13–21] Up to date, various conjugated small molecules and polymers containing such removable solubilizing side groups have been reported. These cleavable groups include Diels-Alder components,[13, 14] silyl groups,[15,16]ester groups,[17–19]keta substituents[20] and *o*-nitrobenzyl (ONB) groups[21]. Most of the required post-processing treatments of these groups, however, either require high temperatures or will leave behind non-volatile residues that lower device performance. The *t*-Butyloxycarbonyl (*t*-Boc) protecting group has demonstrated promise as a cleavable solubilizing functional group because it can be removed at a relatively low temperature (180 °C) as gasous by-products (isobutylene and carbon dioxide). *t*-Boc group has been used to protect latent hydrogen bonds (H-bonds)in organic pigments, such as indigo,[22, 23] quinacridone,[24, 25] and diketopyrrolopyrrole[26]. After the cleavage of *t*-Boc, intermolecular N−H···O=C H-bonds could emerge in the solid-state, affording a robust, insoluble thin film. Herein, we report a side-chain engineering approach to the development of a series of solution processable, semiconducting random copolymers decorated with removable *t*-Boc and solubilizing polyisobutylene (PIB)side-chains. Excellent physical and electronic solvent-resistant properties were demonstrated after thermal treatment.

[a] Department of Chemistry, Texas A&M University, 3255 TAMU, College Station, Texas 77843, United States. Email: fang@chem.tamu.edu
[b] Department of Materials Science and Engineering, Texas A&M University, 3255 TAMU, College Station, Texas 77843, United States.
[c] Beijing National Laboratory for Molecular Sciences, Key Laboratory of Bioorganic Chemistry and Molecular Engineering of Ministry of Education, Center for Soft Matter Science and Engineering, College of Chemistry and Molecular Engineering, Peking University, Beijing 100871, China. Email: jianpei@pku.edu.cn
[d] Department of Chemistry and Biochemistry, University of California, Santa Cruz, 1156 High Street, Santa Cruz, California 95064, United States
Electronic Supplementary Information (ESI) available: [Text giving TGA trace of Monomer 1, FT-IR sepctra of PIIT-Boc65 and PIIT-Boc75, OFET profile of PIIT-Boc70 and PIIT-Boc75, GIXRD pattern of PIIT-Boc70 and PIIT-Boc75 and ^{1}H NMR and ^{13}C NMR of Monomer 1 and Monomer 2].
See DOI: 10.1039/x0xx00000x

Experimental

Synthetic detail

6,6'-dibromoisoindigo[27] and bis(trimethylstannyl)thiophene[28] were synthesized according to procedures reported in the literature. Vinyl group end-functionalized polyisobutylene was purchased from BASF as Glissopal® 1000 (M_n= 1000 g/mol). Other starting materials and reagents were purchased from Aldrich and Alfa-Aesar, and used as received without further purification. Toluene, CH_2Cl_2, DMF and THF were dried through dry Al_2O_3columns and used without further treatment.

Monomer 1: To a solution of 6,6'-dibromoisoinigo (2.25 g, 5.36mmol) in THF (150 mL) was added 4-Dimethylaminopyridine (66 mg, 0.54mmol) and triethylamine (5.40 g, 53.6mmol). The resulting solution was cooled to 0 °C and Boc_2O (2.92 g, 13.4mmol) was added. The reaction mixture was warmed to room temperature, and stirred for 4 h. After quenching with H_2O (100 mL),the reaction mixture was extracted with CH_2Cl_2 (3 × 50 mL).The combined organic layer was dried over $MgSO_4$, filtered through Celite, and concentrated under reduced pressure. The residue was purified by flash column chromatography(SiO_2,hexane/EtOAc, 5:1) to give product **monomer 1**(2.89 g, 87%) as a red solid. ^{1}H NMR (500 MHz, $CDCl_3$): ^{1}H NMR (500 MHz, $CDCl_3$) δ: 8.83 – 8.82 (d, *J* = 8.7 Hz, 2H), 8.06 – 8.05 (d, *J* = 1.9 Hz, 2H), 7.31 – 7.29 (dd, *J* = 8.7, 1.9 Hz, 2H), 1.67 (s, 18H). ^{13}C NMR (125 MHz, $CDCl_3$): δ: 165.5, 148.5, 142.0, 131.9, 130.3, 127.9, 127.4, 120.6, 118.0, 85.7, 28.2.HR-MALDI: calcd for $C_{26}H_{24}Br_2N_2O_6[M\text{-}H]^-$ *m/z* = 618.9899; found *m/z* = 618.9882.

PIB-CH_2-Br: To a mixture of **PIB-CH_2-OH** (24 g, 23.6mmol, M_n = 1018 g/mol) and 200 mL of CH_2Cl_2 was added PPh_3 (7.55 g, 28.8mmol)at room temperature. The resulting solution was cooled to 0 °C and *N*-Bromosuccinimide (5.13 g, 28.8mmol) was added slowly. The resulting reaction mixture was warmed to room temperature, and was stirred for 1 h. The solvent was removed under reduced pressure and the resulting mixture was taken up with 300 mL of hexane, washed with H_2O (3×100 mL). The combined organic layer was dried over $MgSO_4$, filtered through Celite, and concentrated under reduced pressure. The residue was purified by flash column chromatography(SiO_2, hexane) to give product **PIB-CH_2-Br**(21.4 g, 84%) as a sticky oil. The ^{1}H NMR is same as the matched literature report.[35]

Monomer 2: 6, 6'-dibromoisoinigo (1 g, 2.38 mmol) and oven-dried K_2CO_3 (723 mg, 5.24mmol) was mixed in dry DMF (20 mL)in a three-neck flask under the protection of N_2. The mixture was heated at 60 °C for 30 min, before the addition of a solution of **PIB-CH_2-Br** (5.66 g, 5.24 mmol) in dry THF (20 ml) into the reaction mixture dropwise. The temperature was elevated to 90 °C for 12 h to allow the reaction to proceed to completion. The solvent was then removed under reduced pressure and the resulting mixture was taken up with 300 mL of hexane, washed with H_2O (3× 100 mL). The combined organic layer was dried over $MgSO_4$, filtered through Celite, and concentrated under reduced pressure. The residue was purified by flash column chromatography. (SiO_2, hexane /CH_2Cl_2 = 1 : 1) to afford **Monomer 2** (4.03 g, 70%) as a red oil.^{1}H NMR (500 MHz, $CDCl_3$, ppm): δ:9.10 – 9.07 (d, *J*=8.6 Hz,2H), 7.18 –7.15 (dd, *J*= 8.6 Hz, 1.8 Hz, 2H), 6.94 – 6.94 (d, *J* = 1.8 Hz, 2H,), 3.55 – 3.53 (d, *J*= 7.9 Hz, 4H), 1.41 – 1.25 (m, 104H), 1.01 – 0.83 (m, 318H) . ^{13}C NMR (125 MHz, $CDCl_3$): δ 168.29, 146.31, 132.72, 126.87, 125.32, 120.47, 111.81, 105.13, 77.42, 77.16, 76.91, 60.38, 60.03, 59.67, 59.53, 59.31, 58.98, 58.35, 57.04, 48.01, 38.42, 38.30, 38.25, 38.23, 38.15, 37.95, 37.93, 36.04, 32.97, 32.73, 32.56, 32.06, 31.74, 31.38, 31.03, 30.69, 30.32, 29.72, 27.96. (The molecular weight was 3332 g/mol calculated by ^{1}H NMR end group analysis)

General Synthetic Procedure for PIIT-Bocx :**Monomer 1** (y mol), **monomer 2** (x mol), 2,5-bis(trimethylstannyl)thiophene (x+ymol), $Pd_2(dba)_3$ (0.06 eq), P(*o*-tol)$_3$ (0.12 eq) and 15 mL of toluene were added to a Schlenk tube. The tube was charge with nitrogen through a freeze-pump-thaw cycle for three times. The mixture was stirred for 48 h at 100 °C. The mixture was precipitated out in methanol and collected by filtration. The deep blue solid was then washed in the sequence of acetone, hexane and chloroform in a Soxhlet extractor extensively(**PIIT-Boc100** is not soluble in any organic solvent, and **PIIT-Boc65** is fully soluble in hexane). The chloroform solution (**PIIT-Boc75 and PIIT-Boc70**) or hexane solution (**PIIT-Boc65**) was then concentrated by evaporation and precipitated into methanol again. The precipitate was collected by filtration and dried under high vacuum before characterization and device fabrication.

Device fabrication

Top-gate/bottom-contact FET devices were fabricated using n^{++}-Si/SiO_2 (300 nm) substrates. The gold source and drain bottom electrodes (with Ti as the adhesion layer) were patterned by photolithography on the SiO_2 surface. The substrates were subjected to cleaning using ultrasonication in acetone, cleaning agent, deionized water (twice), and isopropanol. The cleaned substrates were dried under vacuum at 80 °C for 2 h. The substrates were transferred into a glovebox. A thin film of the polymer was deposited on the treated substrates by spin-coating using a polymer solution (3 mg/mL in 1,2-dichlorobenzene) at 1500 rpm for 60 s. The as-prepared pristine film was annealed at 180°C for 30 minutes. Both pristine film and annealed films were immersed into different solvents for 5 minutes. Four different active layers were achieved as pristine thin film, pristine thin film immersed in solvent, annealed thin film and annealed thin film immersed in solvent. A CYTOP solution (CTL809M:CT-solv180 = 3:1) was spin-coated onto the semiconducting layer at 2000 rpm for 60 s resulting in a dielectric layer of 500 nm thick. The CYTOP layer was then baked at 100 °C for 1 h. Gate electrodes comprising a layer of Al (50 nm) were then evaporated through

a shadow mask onto the dielectric layer by thermal evaporation.

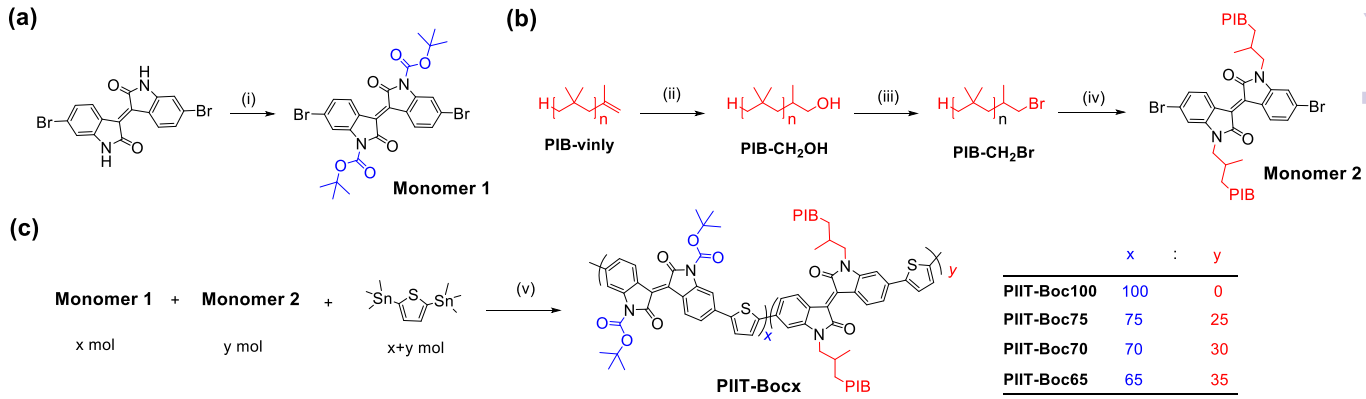

Scheme 1. Synthesis of monomers and random copolymers. (i) DMAP/Et_3N/THF, rt, 4h; (ii) BH_3-SMe_2/Hexane, rt, 24h; then NaOH (aq)/H_2O_2/MeOH, 0°C, 4h; (iii) NBS/PPh_3/CH_2Cl_2, rt, 1h; (iv) 6,6'-dibromoisoindigo/K_2CO_3/DMF/THF, 90°C, 12h; (v) $Pd_2(dba)_3$/P(o-Tol)$_3$/PhMe, 100°C, 48h.

Results and discussion

Molecular Design and Synthesis

Isoindigo-thiophene donor-acceptor polymer[29-34] was chosen as the semiconducting backbone because (*i*) it has showed excellent device performance in organic electronic devices and (*ii*) the feasible functionalization of the nitrogen hetero atom on isoindigo unit.[29]In order to ensure good solubility when a large amount of *t*-Boc groups were serving as the side-chain, polyisobutylene (**PIB**) polymer side-chains were incorporated onto the backbone through random copolymerization. It has already been demonstrated previously that this random copolymerization strategy can render good solubility with a possibly low impact on the electronic performance.[8]

Guided by this design principle, Scheme 1 outlines the syntheses of isoindigo monomers**1** and **2**that are functionalized with *t*-Boc or PIB side-chains, respectively. On one hand, 6,6'-dibromoisoindigo was treated with di-*tert*-butyldicarbonate, catalyzed by dimethylaminopyridine (DMAP) in dichloromethane at room temperature to afford the *t*-Boc functionalized monomer **1**. On the other hand, commercially available vinyl group end-functionalized PIB wasconverted into **PIB-CH_2OH** in a quantitative yield according to the literaturereport.[30] An improved procedure involving Appel reaction was employed to convert **PIB-CH_2OH** into **PIB-CH_2Br** by using NBS as the bromide resource. A mixed solvent of THF and DMF was used for the S_N2 reaction between **PIB-CH_2Br** and 6,6'-dibromoisoindigo to give monomer **2** in 70% yield.

The conjugated statistical copolymers were obtained by palladium-catalyzedStille polymerization of dibromo-monomers **1** and **2** with 2, 5-bis(trimethylstannyl)thiophene at a 1:1 stoichiometric ratio between the overall bromo and trimethylstannyl functional groups. The molar percentage of the PIB and *t*-Boc functionalized repeating units in these copolymers were controlled by the molar ratios of the dibormo-monomers**1** and **2** (Scheme 1). The resulting solubility of these statisticalcopolymers**PIIT-Bocx**(with x implying the molar percentage of Boc functionalized repeating units)varied dramatically depending on the ratio of x. For example, **PIIT-Boc100**could not be dissolved in any common organic solvent. By increasing the molar ratio of PIB functionalized monomer **2** to 25%,the resulting **PIIT-Boc75**couldbe partially dissolved in chloroform. In contrast, the solubility of **PIIT-Boc70 and PIIT-Boc65** was further enhanced to be fully soluble in chloroform as well ashexanes. The molecular weights of these copolymers were evaluated by gel permeation chromatography (GPC) with THF as the eluent and linear polystyrene as standards. The estimated number-average molecular weight (M_n) of **PIIT-Boc75**, **PIIT-Boc70** and **PIIT-Boc65** were 31K, 26K and 32K with polydispersity index (PDI) of 1.7, 1.9 and 2.5, respectively.

Thermal Property

Thermogravimetric analysis (TGA) was conducted to confirm the thermal cleavage property of **monomer 1** and as synthesized ***t*-Boc** protected copolymers. The TGA trace of monomer **1** showed a weight loss (32.5%) at around 180°C corresponding to *t*-Boc cleavage, which is consistent with the theoretical calculated weight percentage of the *t*-Boc groups (32.3%). (Figure. S1) ^{1}H NMR of

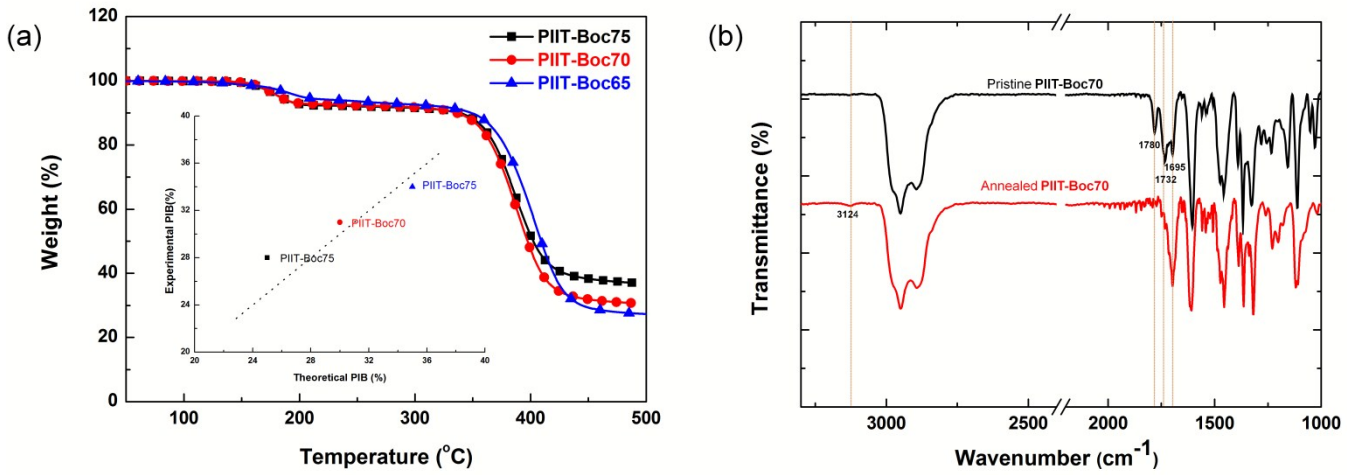

Figure 1.(a) TGA trace of **PIIT-Boc75**, **PIIT-Boc70** and **PIIT-Boc65**; Inset picture indicate the different of PIB containing between experiment and theoretical results (b)FT-IR spectra for the pristine solid and after thermal treatment for **PIIT-Boc70**.

thermally treated monomer **1** showed exactly the same spectra as that of 6**,** 6'-dibromoisoindigo. These results demonstrated that thermolysis of *t*-Boc on isoindigo was highly efficient and the cleavage yielded the de-protected isoindigo unit in aclean manner. The TGA curves of different random copolymers **PIIT-Bocx** are shown in Figure 1a. Two clear steps of weight loss occured at around 180°C and 400°C, which were assigned to the cleavage of the ***t*-Boc** and long **PIB** side-chain, respectively. Based on the weight loss percentage, the ratio of monomer **1** and **2** was calculated and re-examined, which was close to the reaction stoichiometry (inset figure in 1a).

To test the potential solvent-resistant properties, bulk samples of these polymer solids were annealed at 180°C in a vial. The resulting solids could not be dissolved in any solvent including chloroform, DMSO, chlorobenzene, *etc*, on account of the formation of strong intermolecular H-bonds. (Figure S2)

FT-IR Spectroscopy

Fourier transform infrared spectroscopy (FT-IR) was employed to investigate the *t*-Boc cleavage process upon thermal treatment. As shown in Figure 2b, the pristine **PIIT-Boc70** showedthree peaks at 1780 cm^{-1}, 1732 $cm^{-1}$and 1695 cm^{-1}, corresponding to the characteristic C=O stretching in *t*-Boc group, *t*-Boc protected isoindigo unitand PIB side-chain attached isoindigo unit,respectively. After thermal treatment at 180 °C, the C=O stretching of *t*-Boc disappeared, clearly illustrating the removal of Boc groups in the solid. More interestingly, the formation of N–H···O=C H-bonds can be corroborated by the smaller wavenumberof the stretching band of isoindigo C=O, because accepting a H-bond would weaken this C=O bond. In addition, the H-bonding interaction also induced a relatively weak band of the N-H stretching at about 3124 cm^{-1}, which matches literature reported values[22] in other similar structures such as indigoand quinacridone.It was also noteworthy that the characteristic stretching vibration of sp^3 C–H bonds in PIB side-chain ranging from 3100 cm^{-1} to 2800 cm^{-1} remained the same after thermal annealing, in accordance to the TGA result that the PIB chain was stable at the annealing temperature of 180 °C.

Photophysical and Electrochemical Properties

The UV-Vis spectra of **PIIT-Boc75**, **PIIT-Boc70** and **PIIT-Boc65** in dichloromethane solution, pristine film and thermal annealed films are shown in Figure 2. All three polymers showed similar features with two absorption bands, which could be attributed to π-π* absorption (band from 400 nm to 500 nm) and donor-acceptor chargetransfer (CT) absorption from electron-rich thiophene to elector-deficient isoindigo (broad

Table 1. Molecular weight and photophysical properties of random conjugated copolymer. Properties of the annealed films properties are in parentheses.

Polymer	Mn (kg·mol$_{-1}$)	PDI	E_{HOMO}(eV)[a]	E_{LUMO}(eV)[a]	E_g^{opt}(eV)[a]	E_g(eV)[b]
PIID-Boc75	31.0	1.7	-5.35 (-5.40)	-3.64 (-3.55)	1.71 (1.85)	1.51 (1.54)
PIID-Boc70	26.0	1.9	-5.42 (-5.39)	-3.72 (-3.59)	1.70 (1.80)	1.51 (1.55)
PIID-Boc65	32.0	2.5	-5.36 (-5.35)	-3.62 (-3.55)	1.74 (1.80)	1.51 (1.59)

a. Energy level calculated from CV measurement. Electrolyte: 0.1 M TBAPF6 in CH_3CN. Potential calculated versus Fc/Fc^+. Scan rate: 50 mV/s; b. Optical band gap calculate from UV onset..

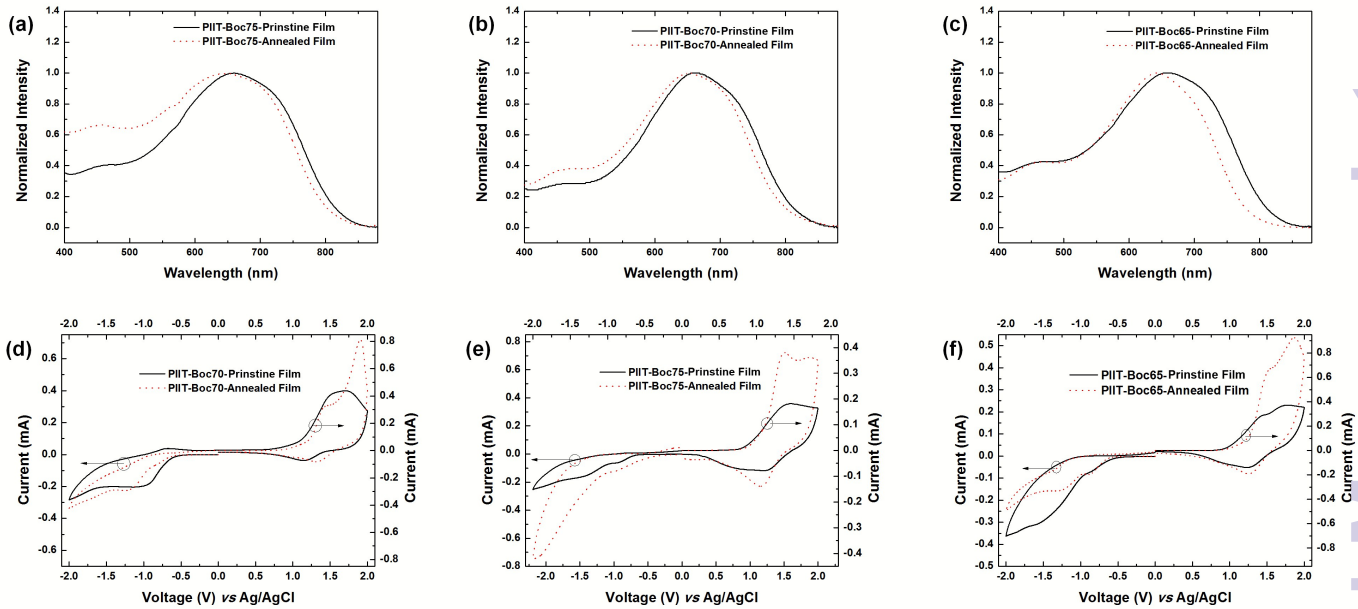

Figure 2. Uv-*vis* spectra of (a) **PIIT-Boc75**, (b) **PIIT-Boc70** and (c) **PIIT-Boc65** before and after thermal annealing; Cyclicvoltammetry trace of (d) **PIIT-Boc75**, (e) **PIIT-Boc70** and (f) **PIIT-Boc65** before and after thermal annealing.

band from 500 nm to 850 nm).[27] Due to the bulky nature of ***t*-Boc** group and **PIB** side-chain, the film absorption was only slightly red shifted compared to that in solution, because the π-π stacking in the solid state was relatively weak. After thermal treatment, the absorption of all three polymers were blue-shifted compared to the pristine films. This blue-shift can be attributed to H-bond alternated resonance contribution or an enforced twisted torsional conformation that possesses shorter effective conjugated length. This phenomenon was also seen in other reported thermal cleavage conjugated polymers.[22,24]Interestingly, the larger blue-shift was observed while the higher PIB ratio was in the polymer chain. For example, compared to the pristine film, the blue shifts of annealed **PIIT-Boc75**, **PIIT-Boc70** and **PIIT-Boc65**were 15 nm, 20 nm and 36 nm, respectively. We deduced that the remaining bulky PIB side-chain could disrupt the π-π stacking and disorder the polymer backbone arrangement in a compact polymer network. Thus, the more PIB remaining, the larger blue shift was observed.

Electrochemical properties of the polymer films before and after thermal treatment were investigated using cyclicvoltammetry (CV). The measurements were carried out under an inert atmosphere by using tetra-*n*-butylammoniumhexafluorophosphate (n-Bu_4NPF_6, 0.1 M in acetonitrile) as the supporting electrolyte with an indium tin oxide (ITO) glass working electrode, a platinum wire counter electrode, and a Ag/AgCl electrode as reference electrode. The potential of the ferrocene/ferrocenium (Fc/Fc^+) redox couple was measured as a standard. The ITO was employed because it is feasible to process the annealing process. The results are shown in Figure 2 and the corresponded energy level is summarized in Table 1. The E_{HOMO} levels of pristine films and annealed films are almost the same while the E_{LUMO} levels of annealed films are approximately 0.1 eV higher than that of pristine films, resulting in larger band gaps for annealed films. For example, before and after annealed, the E_{HOMO}s of **PIIT-Boc70** were –5.42 eV and –5.39 eV while the E_{LUMO}s were –3.72 eV and –3.59 eV, respectively. This trend agreed well with the corresponding UV/vis spectra, from which the optical bandgaps were calculated from the absorption onset.

Solvent Resistance Test and Multilayer Film Processing

Because of the formation of intermolecular H-bonds after thermal cleavage of *t*-Boc, the annealed thin film became solvent resistant. Most reported solution-processed thin films of conjugated polymers are soluble in similar organic solvents. This problem represents a major challenge for multilayer device fabrication using solution-processing techniques. The post-treatment induced solvent resistance demonstrated in this system would be an ideal strategy to address this issue. For a proof-of-concept, solution castingof multiple layers of **PIIT-Boc70**through a "casting-annealing-casting-annealing" cycles was conducted. We performed spin-casting of a solution of **PIIT-Boc70** in$CHCl_3$ onto a glass substrate following by thermal annealing at 180 °Cfor 10 min. This procedure was repeated for 5 times to afford a film 6 times thicker than that was cast from one single cycle (Figure 3). The UV-vis spectra showed the absorption of the thin film increased linearly as the number of layers increased (Inset in Figure 3). In principle, this process can be repeated for multiple times with either the

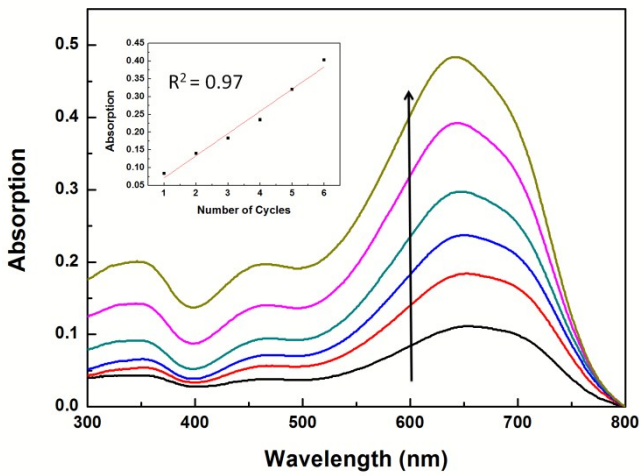

Figure 3. Uv-vis spectra of **PIIT-Boc70**film by casting-annealing-casting-annealing" cycles (Inset picture: the relationship between number of cycles and absorption in 600 nm).

same polymerfor potential fabrication of uniform thicker films, or different polymer for multilayer film fabrication.

OFET

Top-gate/bottom-contact (TG/BC) device structure was used to test the carrier transport property of **PIIT-Boc75** and **PIIT-Boc70** both in pristine and annealed films. As shown in figure S15, the active layer was deposited by spin-coating a polymer solution (3 mg / mL in DCB) onto Au (source-drain) / SiO_2 / Si substrate. The annealed active layer was obtained by heating the film at 180°C for 30 minutes. As mentioned before, these polymer films have an excellent solvent-resistant property after thermal treatment. In order to study the solvent resistant property of these thin films in terms of electronic properties, both pristine film and annealed films were immersed into different solvents for 5 minutes. Subsequently, a CYTOP solution was spin-cast onto the top of the four different types of active layers and cross-linked under 100 °C for 1 h, forming the dielectric layer. Then, 80 nm aluminumlayer was vacuum deposited as the gate electrode. Figure 4 and Figure S5–S14illustrate the transfer and output curve of**PIIT-Boc75**and **PIIT-Boc70** as pristine film, annealed film and solvent immersed annealed film. The device performance results are summarized in Table 2 and Table S1–S2. They all showed typical *p*-type characteristic under ambient condition. Mobility of the pristine thin films of **PIIT-Boc75** and **PIIT-Boc70** were1.61 × 10^{-4}cm^2 V^{-1}s^{-1} and 9.67 × 10^{-5} cm^{2}V^{-1}s^{-1} respectively. After thermal treatment, the annealed device mobility of **PIIT-Boc75** and **PIIT-Boc70**were slightly higher (2.15 × 10^{-4} cm^2 V^{-1}s^{-1} and 2.02 × 10^{-4} cm^2 V^{-1}s^{-1}, respectively).

After being immersed in solvents, the pristine and annealed devices showed drastically different performances (Table 2). For the immersed pristine film devices, mobility of **PIIT-Boc75** dramatically decreased because the film was probably partially dissolved and damaged in organic solvents. Furthermore, the mobility of **PIIT-Boc70**thin film could not be measured because the pristine film was completely dissolved into the solvent. For the immersed annealed devices, however, either **PIIT-Boc75** or **PIIT-Boc70** showed consistent OFET device performance compared to the not immersed ones. These results demonstrated that the annealed thin films not only could keep the physical presence in the presence of solvent etching, but also could retain the electronic properties.This unique solvent resistant property makes this kind of intermolecular H-bonding materials a good candidate applicable in multi-layer solution processing of thin films.

Morphology and GIXD

To further illustrate the morphology and molecule packing of the solvent resistant films, grazing incidence X-ray diffraction (GIXRD) analysis was carried for **PIIT-Boc75** and **PIIT-Boc70** both in pristine film and annealed film. As shown in figure 5a, the as-cast **PIIT-Boc75** pristine film had two characteristic peaks in the out of plane direction, corresponding to the PIB lamellar packing (1.15 A^{-1}, 5.46 Å) and π-π stacking distance between the polymer backbone (1.79 A^{-1}, 3.51 Å). After thermal annealing, the π-πdistance was slightly increased (1.75 A^{-1}, 3.59 A). This result was consistent with the slightly blue shifted UV-vis spectra, which indicated a twisted torsional conformation and consequently enlarged intermolecular π-π stacking distance. Interestingly, the as-cast **PIIT-Boc70** pristine film showed a different feature: Only one broad peak was observed, suggesting an amorphous nature of this film. This morphology corresponds to the increased amorphous PIB side-chains ratio on the polymer backbone. After thermal treatment, however, the intermolecular H-bonds network increased the crystallinity of **PIIT-Boc70,** leading to two characteristic peaks consistent with the result of the annealed **PIIT-Boc75** film.

Table 2.OFET property of **PIID-Boc75** and **PIID-Boc**70 for four different type devices by using TG/BC device structure.

	Pristine Thin Film		Pristine Thin Film Immersed in Solvent		Annealed Thin Film		Annealed Thin Film Immersed in Solvent	
	μ ($cm^2V^{-1}s^{-1}$)	V_{th}(V)	μ ($cm^2V^{-1}s^{-1}$)	V_{th}(V)	μ ($cm^2V^{-1}s^{-1}$)	V_{th}(V)	μ ($cm^2V^{-1}s^{-1}$)	V_{th}(V)
PIID-PIB25-Boc75	1.61E-04	1.98	7.22E-05	7.40	1.09E-04	13.22	1.38-04[e]	23.69[e]
PIID-PIB30-Boc70	9.67E-05	29.31	N.A	N.A	2.02E-04	30.15	1.62E-04[e]	27.30[e]

a. Pristine device; b. Immersed pristine device; c. Annealed device; d. Immersed annealed device; e. Immersed the annealing film in $CHCl_3$ for 5 min at room temperture.

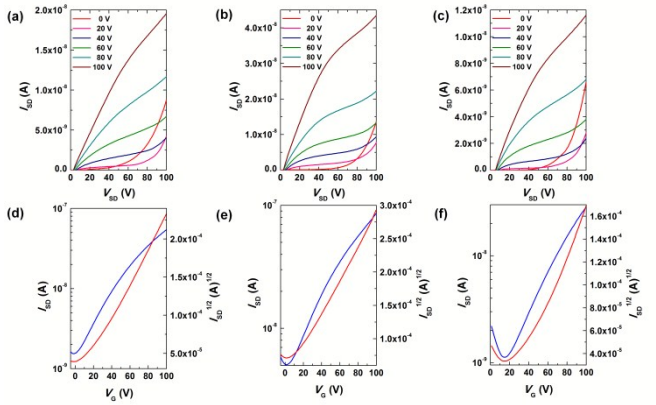

Figure 4. Output curves of **PIIT-Boc75** in (a) pristine film, (b) annealed film and (c) immersed annealed film($CHCl_3$); Transfer curves of **PIIT-Boc75** in (d) pristine film, (e) annealed film and (f) immersed annealed film ($CHCl_3$).

The effect of thermal treatment on the surface morphology of random copolymer films was also examined by atomic force microscopy(AFM). All the samples were prepared using the same condition as device fabrication, followed by thermal treatment at 180 C for 10 min and immersing in $CHCl_3$ for 5 min at room temperature. As shown in Figure 5b, by increasing the ratio of amorphous PIB chains on polymer backbones, smoother surfaces of pristine films were achieved. For example, root-mean-square roughness (RMS) value was 2.27 nm for **PIIT-Boc75** compared to only 0.56 nm for **PIIT-Boc65**. This differencewas likely the result of combined two effects: (1) the stronger amorphous nature of more PIB chains in **PIIT-Boc65** and (2) less aggregation during film processing when the solubility was higher. After thermal treatment, lower RMS values of annealed films were achieved for all three polymer films compared to the pristine film. Meanwhile, more aggregation areas were observed in anneal film, which is consistent to the GIXR results. AFM study has also been conducted on the thin films immersed in different organic solvents after annealing. Because of the excellent solvent resistant nature of the annealed polymer, the morphology of the immersed films remained the same and RMS values were only slightly increased in comparison to the pristine films. This consistent morphology of the films before and after thermal treatment guaranteed the consistent electronic properties for the previously discussed OFET devices.

Conclusions

In summary, a series of solution processable semiconducting polymers with latent H-bond ability were synthesized through a statistical copolymerization approach. After solution casting, regeneration of intermolecular H-bonds was achieved by cleavage of the *t*-Boc groups under a mild thermal annealing condition. Through this unique side-chain engineering approach, the resulting thin film demonstrated excellent solvent resistance in both terms of physical and electronic properties. This approach is intrinsically versatile so that it can be employed to access polymeric materials applicable in

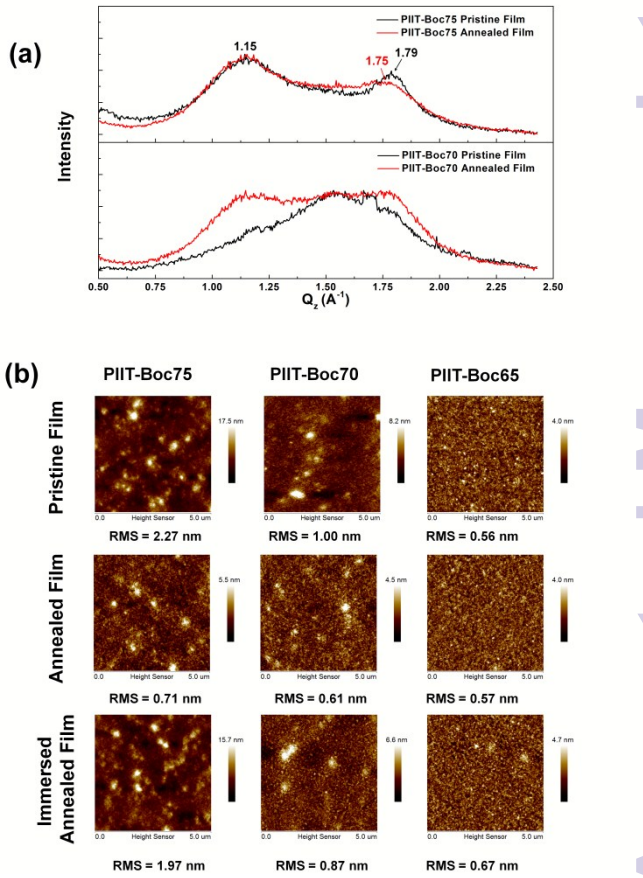

Figure 5. (a) Out of plan GIXRD file of pristine (black) and annealed (red) polymer films; (b) AFM imagine of pristine films, Annealed films and immersed films ($CHCl_3$).

solution-processed multiple-layer electronic devices and direct-contacting sensor in organic solutions.

Acknowledgements

We thank the Donors of the American Chemical Society Petroleum Research Fund (through PRF# 54249-DNI7) and Texas A&M University for support of this research. We also thank Dr. Yuwei Kan for the helping of Thermogravimetric analysis and Dr. Fei Li for the helping of cyclicvoltammetry test.

Notes and references

1 Y. Tao, C. Yang and J. Qin, *Chem. Soc. Rev.*, 2011, **40**, 2943–2970.
2 H. Uoyama, K. Goushi, K. Shizu, H. Nomura and C. Adachi, *Nature*, 2012, **492**, 234–238.
3 L. Yao, S. Zhang, R. Wang, W. Li, F. Shen, B. Yang and Y. Ma, *Angew. Chem. Int. Ed.*, 2014, **53**, 2119–2123.
4 H. -R. Tseng, H. Phan, C. Luo, M. Wang, L. A. Perez, S. N. Patel, L. Ying, E. J. Kramer, T. -Q. Nguyen, G. C. Bazan and A. J. Heeger, *Adv. Mater.*, 2014, **26**, 2993–2998.
5 X. Zhou, N. Ai, Z. -H. Guo, F. -D. Zhuang, Y. -S. Jiang, J. -Y. Wang and J. Pei, *Chem. Mater.*, 2015, **27**, 1815−1820.

6 Y. Cao, Z. -H. Guo, Z. -Y. Chen, J. -S. Yuan, J. -H. Dou, Y. -Q. Zheng, J. -Y. Wang and J. Pei, *Polym. Chem.*, 2014, **5**, 5369–5374.
7 Y. Huang, E. J. Kramer, A. J. Heeger and G. C. Bazan, *Chem. Rev.*, 2014, **114**, 7006−7043.
8 L. Fang, Y. Zhou, Y. -X. Yao, Y. Diao, W. -Y Lee, A. L. Appleton, R. Allen, J. Reinspach, S. C. B. Mannsfeld and Z. Bao, *Chem. Mater.*, 2013, **25**, 4874−4880.
9 J. You, L. Dou, K. Yoshimura, T. Kato, K. Ohya, T. Moriarty, K. Emery, C. -C. Chen, J. Gao, G. Li and Y. Yang, *Nat. Commun.*, 2013, **4**, 1446.
10 A. J. Heeger, N. S. Sariciftci and E. B. Namdas,*Semiconducting and Metallic Polymers*, Oxford University Press, 2010.
11 A. C. Arias, J. D. MacKenzie, I. McCulloch, J. Rivnay and A. Salleo, *Chem. Rev.*, 2010, **110**, 3–24.
12 T. Lei, J. -H. Dou and J. Pei, *Adv. Mater.*, 2012, **24**, 6457–6461.
13 C. Liu, W. Xu, X. Guan, H. -L. Yip, X, Gong, F. Huang and Y. Cao, *Macromolecules*, 2014, **47**, 8585−8593.
14 T. Uemura, M. Mamada, D. Kumaki and S. Tokito, *ACS Macro Lett.*, 2013, **2**, 830−833.
15 S. Jakob, A. Moreno, X. Zhang, L. Bertschi, P. Smith, A. D. Schlüter and J. Sakamoto, *Macromolecules*, 2010, **43**, 7916–7918.
16 E. Bundgaard, O, Hagemann, M. Bjerring, N. C. Nielsen, J. W. Andreasen, B. Andreasen and F. C. Krebs, *Macromolecules*, 2012, **45**, 3644−3646.
17 M. Helgesen, S. A. Gevorgyan, F. C. Krebs and R. A. Janssen, *Chem. Mater.*, 2009, **21**, 4669–4675.
18 Y. Liu, S. R. Scully, M. D. McGehee, J. Liu, C. K. Luscombe, J. M. J. Fréchet, S. E. Shaheen and D. S. Ginley, *J. Phys. Chem. B*, 2006, **110**, 3257-3261.
19 B. Sun, W. Hong, H. Aziz and Y. Li, *J. Mater. Chem.*, 2012, **22**, 18950–18955.
20 C. B. Nielsen, E. -H. Sohn, D. -J. Cho, B. C. Schroeder, J. Smith, M. Lee, T. D. Anthopoulos, K. Song and I. McCulloch. *ACS Appl. Mater. Interfaces*, 2013, **5**, 1806−1810.
21 Z. C. Smith, D. M. Meyer, M. G. Simon, C. Staii, D. Shukla and S. W. Thomas, *Macromolecules*, 2015, **48**, 959−966.
22 C. Liu, S. Dong, P. Cai, P. Liu, S. Liu, J. Chen, F. Liu, L. Ying, T. P. Russell, F. Huang and Y. Cao, *ACS Appl. Mater. Interfaces*, 2015, **7**, 9038−9051.
23 E. D. Głowacki, G. Voss, K. Demirak, M. Havlicek, N. Sünger, A. C. Okur, U. Monkowius, J. Gąsiorowski, L. Leonat and N. S. Sariciftci, *Chem. Commun.*, 2013, **49**, 6063−6065.
24 M. Sytnyk, E. D. Głowacki, S. Yakunin, G. Voss, W. Schöfberger, D. Kriegner, J. Stangl, R. Trotta, C. Gollner, S. Tollabimazraehno, G. Romanazzi, Z. Bozkurt, M. Havlicek, N. S. Sariciftci and W. Heiss, *J. Am. Chem. Soc.*, 2014, **136**, 16522–16532.
25 K. Yang, T. He, X. Chen, S. Z. D. Cheng and Y. Zhu, *Macromolecules*, 2014, **47**, 8479−8486.
26 J. Lee, A. -R. Han, J. Hong, J. H. Seo, J. H. Oh and C. Yang, *Adv. Funct. Mater.*, 2012, **22**, 4128–4138.
27 J. Mei, K. R. Graham, R. Stalder and J. R. Reynolds, *Org. Lett.*, 2010, **12**, 660–663.
28 G. Zhang, Y. Fu, Z. Xie and Q. Zhang, *Macromolecules*, 2011, **44**, 1414–1420.
29 T, Lei, J. -Y. Wang and J. Pei, *Acc. Chem. Res.*, 2014, **47**, 1117−1126.
30 J. Mei, H. -C. Wu, Y. Diao, A. Appleton, H. Wang, Y. Zhou, W. -Y. Lee, T. Kurosawa, W. -C. Chen and Z. Bao, *Adv. Funct. Mater.*,2015, **25**, 3455–3462.
31 J. Mei, D. H. Kim, A. L. Ayzner, M. F. Toney and Z. Bao, *J. Am. Chem. Soc.*, 2011, **133**, 20130–20133.
32 R. Stalder, C. Grand, J. Subbiah, F. So and J. R. Reynolds, *Polym. Chem.*, 2012, **3**, 89–92.
33 L. A. Estrada, R. Stalder, K. A. Abboud, C. Risko, J. -Luc. Brédas and J. R. Reynolds, *Macromolecules*, 2013, **46**, 8832−8844.
34 E. Wang, Z. Ma, Z. Zhang, K. Vandewal, P. Henriksson, O. Inganäs, F. Zhang and M. R. Andersson, *J. Am. Chem. Soc.*, 2011, **133**, 14244–14247.
35 J. Li, S. Sung, J. Tian and D. E. Bergbreiter, *Tetrahedron*,2005, **61**,12081–12092.

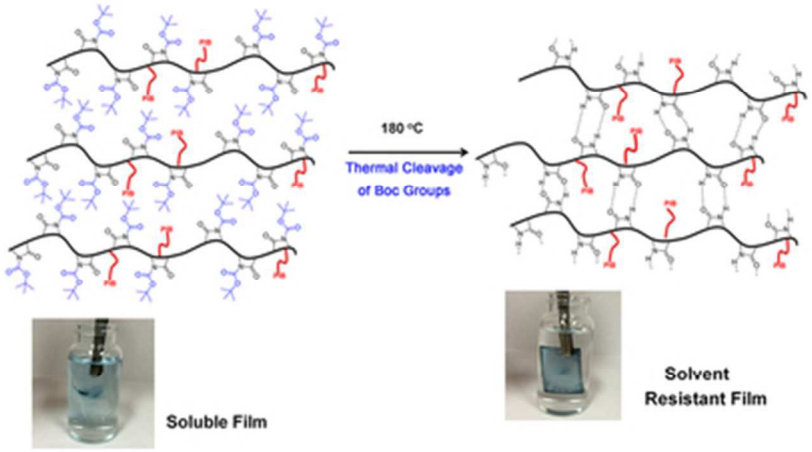

39x19mm (300 x 300 DPI)